Explicitly-Coupled Cloud Physics and Radiation Parameterizations and Subsequent Testing in HWRF

Gregory Thompson[1], Ligia Bernardet[2], Mrinal Biswas[1], Christina Holt[2]

NOAA & NCAR Developmental Testbed Center (DTC)

[1]Research Applications Laboratory
National Center for Atmospheric Research
Boulder, CO, USA

[2]University of Colorado, CIRES
NOAA - Earth Systems Research Laboratory (ESRL/GSD)
Boulder, CO, USA

17 Dec 2014

Motivation

Nearly two years ago, the first attempts to run the Thompson et al. (2008) microphysics scheme in HWRF revealed that only the cloud water and cloud ice species were being treated as "clouds" in the GFDL radiation scheme. Due to the explicit (bin scheme) transfer function from cloud ice to snow, immediately starting at 200 microns, the cloud ice mass mixing ratio in Thompson regularly has one-tenth the values typically found in all other bulk microphysics parameterizations (BMP). However, the combined mass mixing ratio of cloud ice and snow is usually very nearly the same in various BMPs and GFDL radiation scheme does not consider the snow mixing ratio when doing longwave and shortwave radiation fluxes. Therefore, the very low cloud ice amount in Thompson made deep ice/snow clouds far too transparent. Sample HWRF simulation showing outgoing, top-of-atmosphere longwave radiation with operational (Ferrier & GFDL) versus test (Thompson & GFDL) physics clearly illustrates the problem in Fig. 1. Similarly, the incoming solar radiation reaching the surface was far too great in regions of heavy snow (KS, OK, MO, IL) during a blizzard event simulated by HWRF, shown in Fig. 2. ***Summary: Ice/snow clouds in Thompson+GFDL are nearly transparent.***

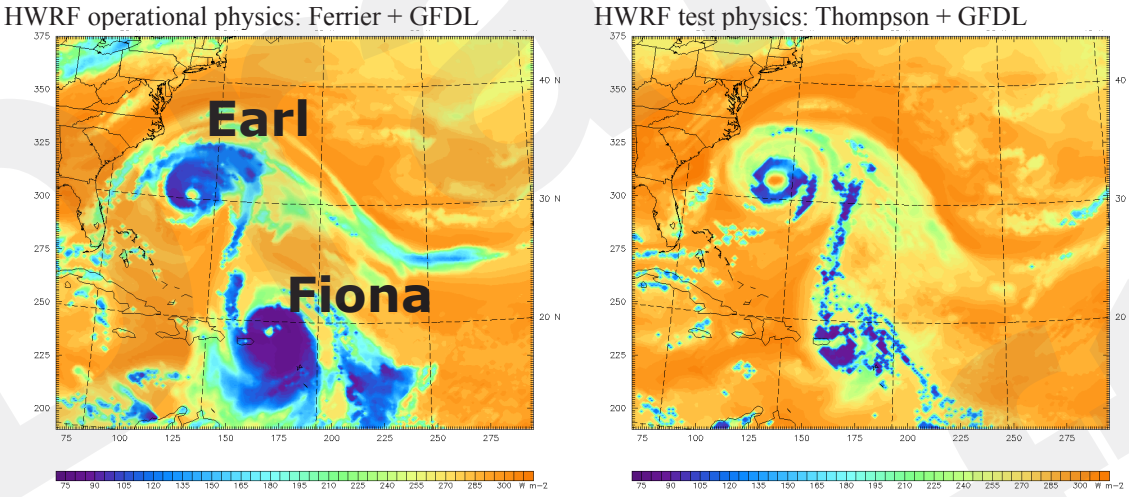

Fig. 1: Outgoing, top-of-atmosphere longwave radiation from 126-h HWRF simulations valid 18z 02Sep2010 using operational (left) and test (right) physics packages.

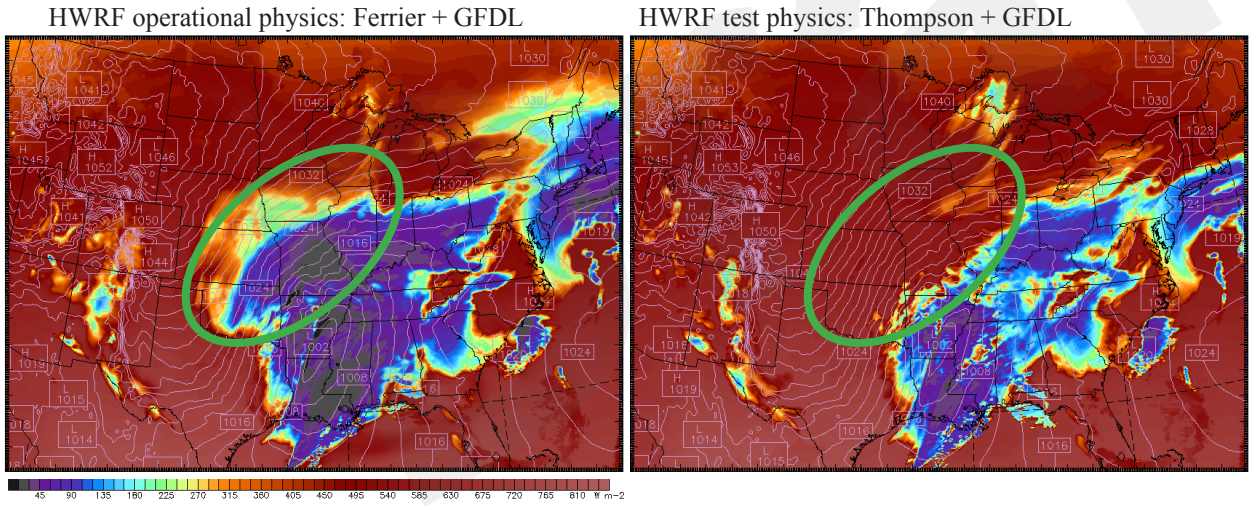

Fig. 2: Incoming solar (shortwave) radiation reaching the ground from 18-h HWRF simulations valid 18z 01Feb2011 using operational (left) and test (right) physics packages. In reality, a blizzard has begun to form and move from near Oklahoma City to Chicago and both schemes had plenty of snow. It is simply that GFDL radiation in HWRF is ignoring this variable.

More recently, DTC visitors Robert Fovell and Peggy Bu (UCLA) provided ample evidence (Bu et al. 2014) that the GFDL radiation scheme in HWRF does not produce the proper feedbacks of temperature tendencies by clouds, i.e., the longwave cooling at cloud top and the shortwave heating by absorption of solar radiation. Simultaneously, Greg Thompson and Mukul Tewari at NCAR-RAL created the connection of the RRTMG radiation scheme together with the explicitly-predicted radiative effective radii of cloud water, cloud ice, and snow variables within the Thompson et al. (2008) microphysics scheme. [This represented highly leveraged work with DTC and another NCAR project and was released to the public in Aug. 2013 as part of WRF v3.5.1.] Furthermore, with a relatively small amount of additional work, nearly any other BMP could pass its explicitly-calculated cloud water, cloud ice, and snow effective radii from any other BMP directly to RRTMG, because currently only the combination of Thompson & RRTMG is enabled in this manner. Without this explicit coupling, the RRTMG implemented into WRF has a priori assumptions of water droplet and ice crystal sizes that are not remotely related to specific assumptions made by the BMP, specifically, droplet or ice/snow spectral distribution nor mass-diameter relations - both of these greatly impact the effective radii and subsequent cloud optical depth and final radiation fluxes. To illustrate, a re-run of the simulations shown in Figs. 1-2 was performed, first with the "standard" RRTMG scheme (uncoupled cloud physics variables) and, then, after the explicitly-computed effective radii of cloud water, cloud ice, and snow were included. These results are shown in Figs. 3-4. Comparing the right-side of Fig. 3 to the same panel of Fig. 1, note how the new combination of physics affected the storm center location of Earl significantly westward - a good outcome for this storm. Also note the dramatic differences with appearance of Fiona, in which the operational physics is likely producing a much more intense tropical cyclone compared to observations whereas the results with Thompson microphysics may be producing too weak a storm. ***Summary: 1) Radiation and cloud physics both have impacts to TC track/intensity. 2) Ice/snow clouds in Thompson+RRTMG are more appropriately taken into account and they create known connections to physical temperature tendencies. 3) Fully coupled water droplet and ice crystals sizes provide physical consistency and opportunity to simulate well-known cloud-radiative "indirect effects," which is a major climate connection research problem.***

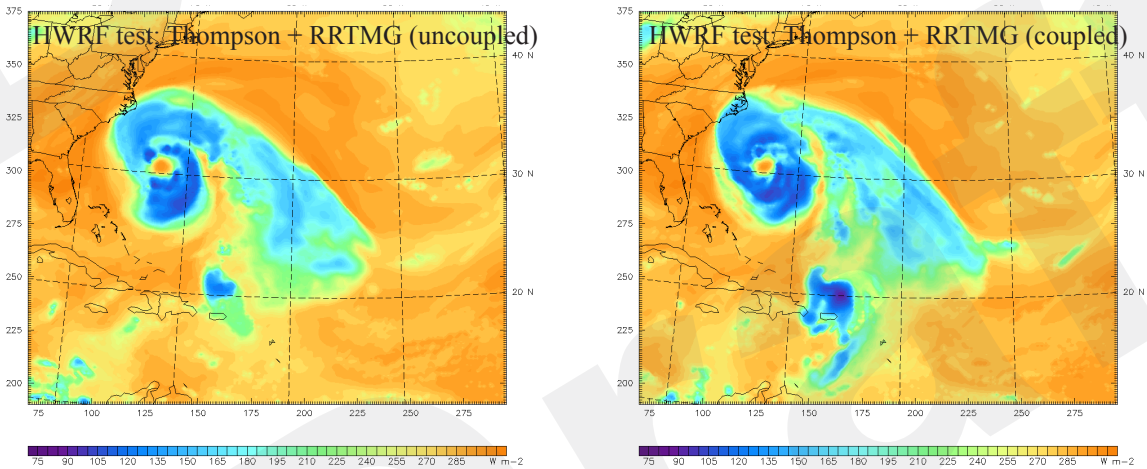

Fig. 3: Same as Fig. 1b except using RRTMG (uncoupled) (left) and fully-coupled RRTMG radiation scheme.

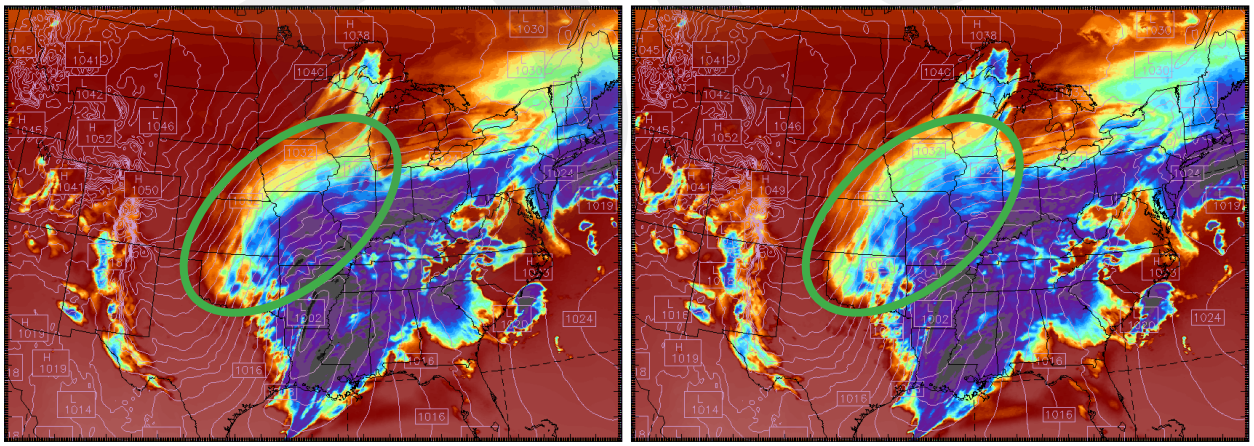

Fig. 4: Same as Fig. 2b with Thompson and uncoupled RRTMG (left) and coupled RRTMG (right).

Next step: Does combining physics improve T.C. characteristics?

With the completion of the combined new physics packages in 2013, are tropical cyclone track, intensity, or other characteristics improved? Initially: yes and no. A DTC test of numerous 2012 Atlantic and Pacific basin storms reveals mixed results. There was an improvement to the longer-term (48-108 h) Atlantic storm characteristics. However, there was also a systematic degradation to nearly all East Pacific storms. This is best seen in the summary graphic below in Fig. 5.

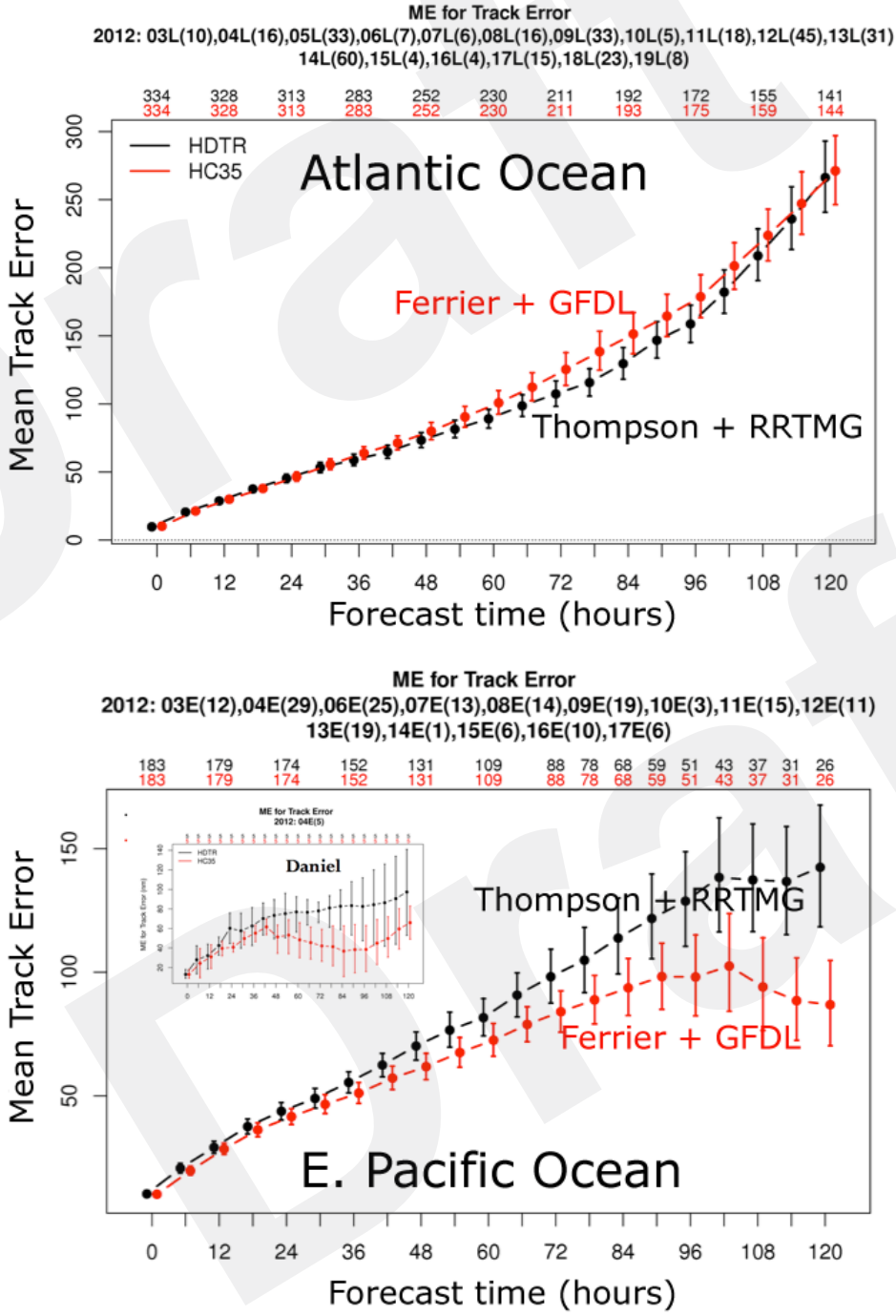

Fig. 5: Mean track error of numerous HWRF 2012 tropical cyclone forecasts in the Atlantic and East Pacific basins. The inset in the lower panel shows Daniel, which typifies the error found in many E-Pac storms and is therefore investigated more throroughly in future test simulations.

E-Pac Daniel

Since the Atlantic basin results with new physics didn't suffer any serious degradation that was found in the East Pacific, a deeper investigation immediately began with a concentrated focus on extent of cloudiness, because one of the primary differences in these two basins is the dominant presence of boundary layer stratus and stratocumulus clouds found in both hemispheres over the eastern Pacific Ocean. The following sequence of visible satellite images from GOES-West taken on subsequent days at 1800 UTC from 04-08 July 2012 clearly shows Daniel and the prevalence of stratus clouds well away from the storm location, but incredibly persistent the entire period (see Figs. 6-7).

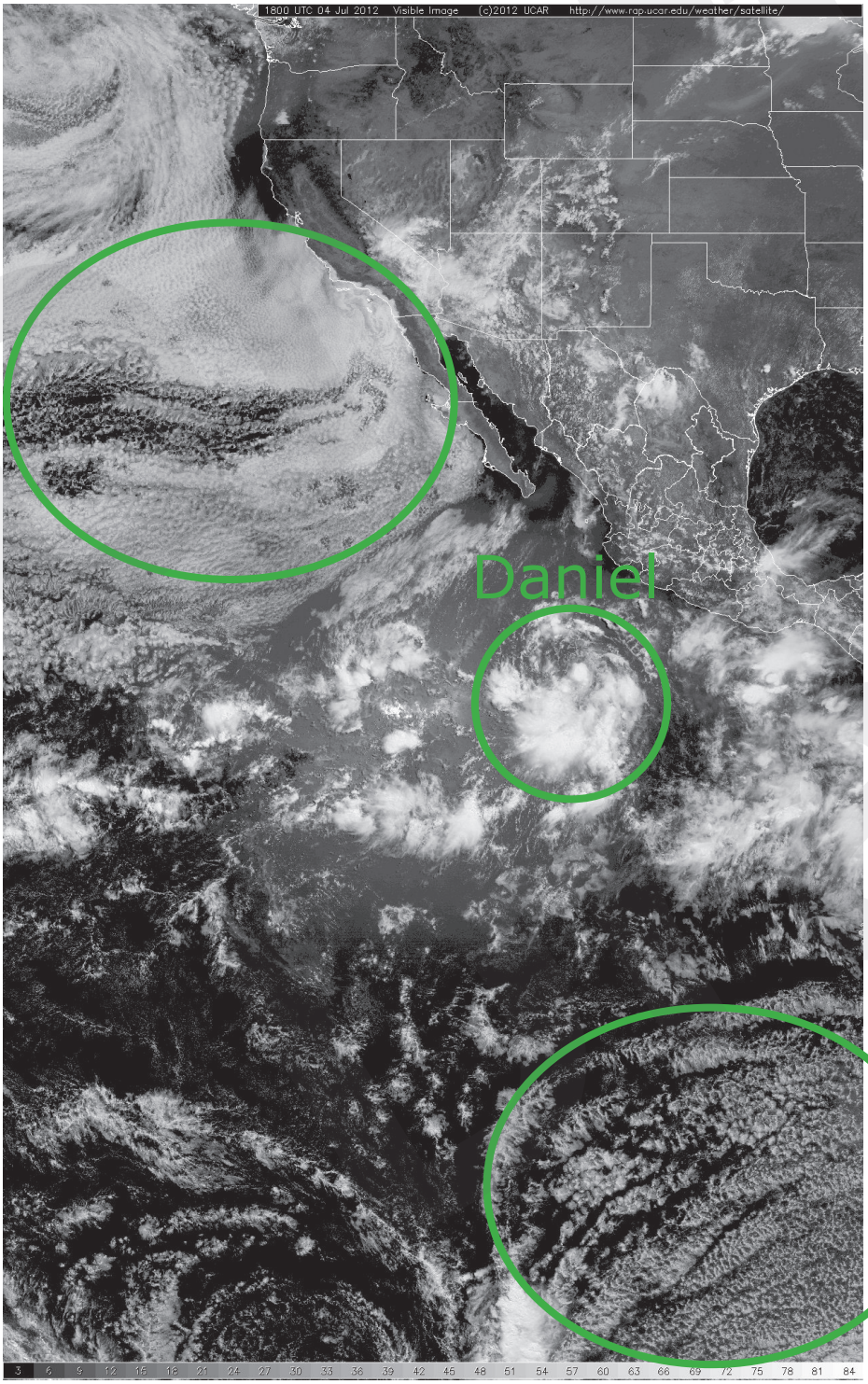

Fig. 6: GOES-West visible (ch1) satellite image valid at 1800 UTC 07 Jul 2012. Note the beginning of tropical cyclone Daniel and the extensive stratus and stratocumulus clouds in both the northern and southern hemisphere. The medium brightness region slightly to the west of Daniel is sun-glint off the ocean surface as well as some cloudiness.

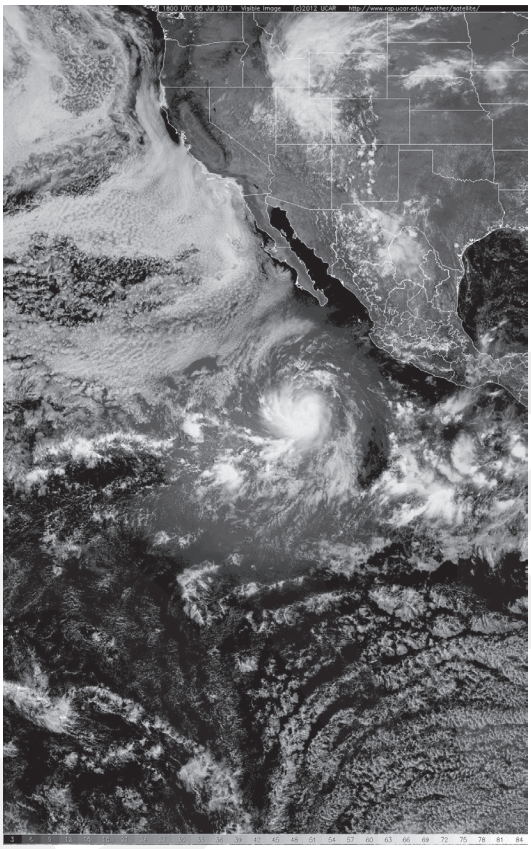

Fig. 7: Same as Fig. 6 except: 1800 UTC 05 Jul (top-left), 1900 UTC 06 Jul (top-right), 1800 UTC 07 Jul (lower-left), and 1800 UTC 08 Jul (lower-right).

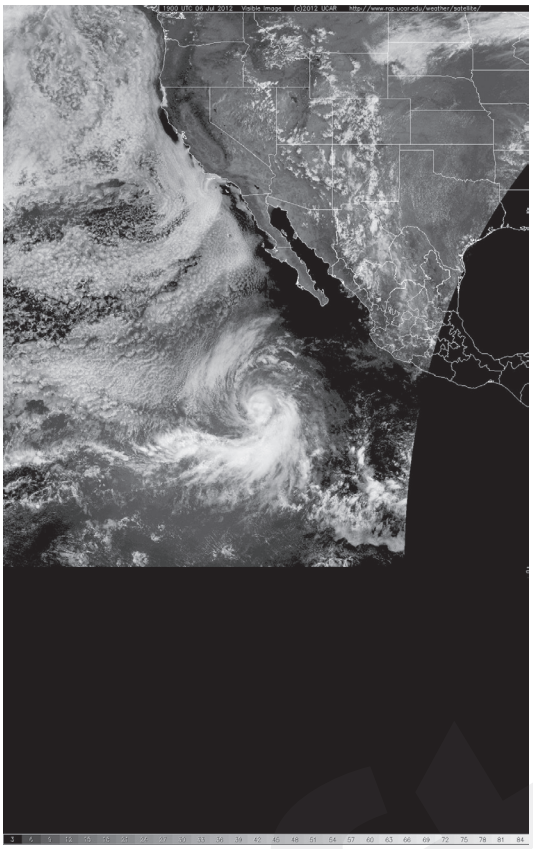

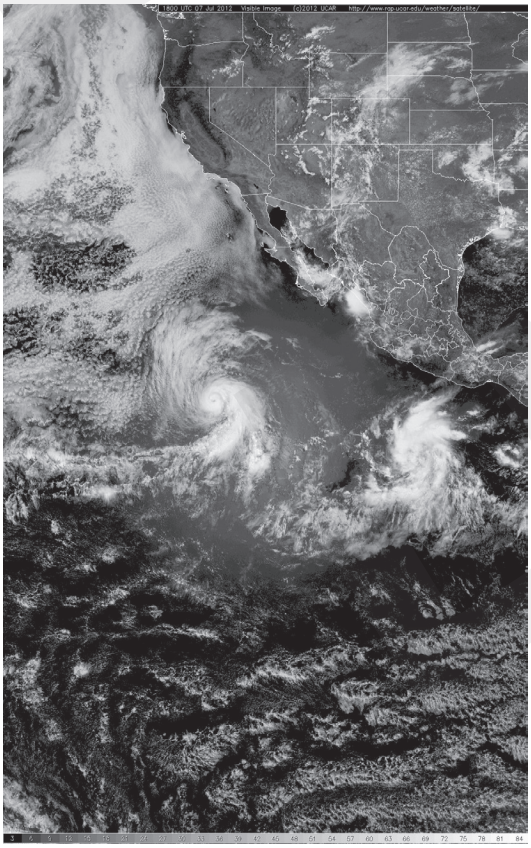

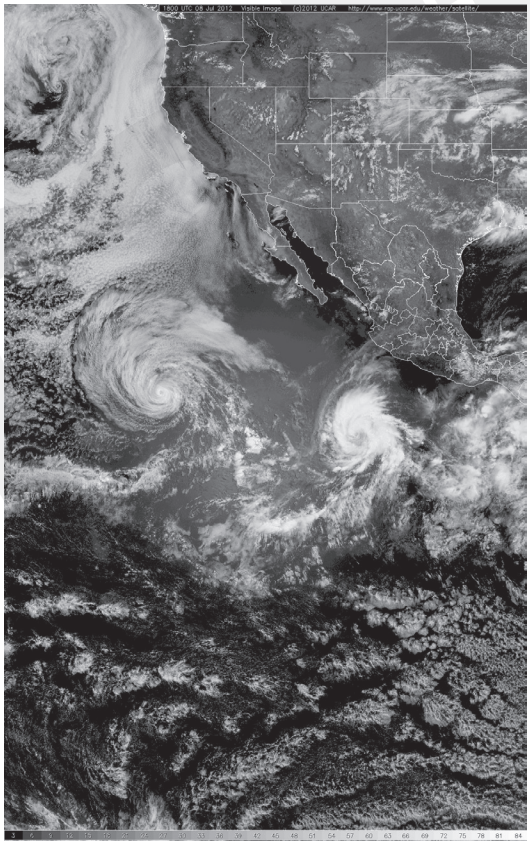

The Cloud Connection

A relatively quick glimpse into the operational versus test physics results of Daniel showed very similar patterns, amounts, and placement of total precipitation as well as its constituent components: explicit (grid-resolved microphysics) and convective parameterization (SAS, in this case) precipitation regardless of physics changes from Ferrier & GFDL to Ferrier & RRTMG, or Thompson & RRTMG (see Fig. 8). While the exact amounts between these sensitivity experiments do show differences, what we will subsequently show is that what matters most is the differentiation between the two purple color shades shown at the bottom of the color scale. Note the darker purple color indicates a precipitation amount larger than zero and how widespread it can be found in the southern Pacific Ocean due to the convective parameterization (middle row). Also note the extremely limited extent of grid-resolved precip (microphysics scheme) in any of the sensitivity experiments.

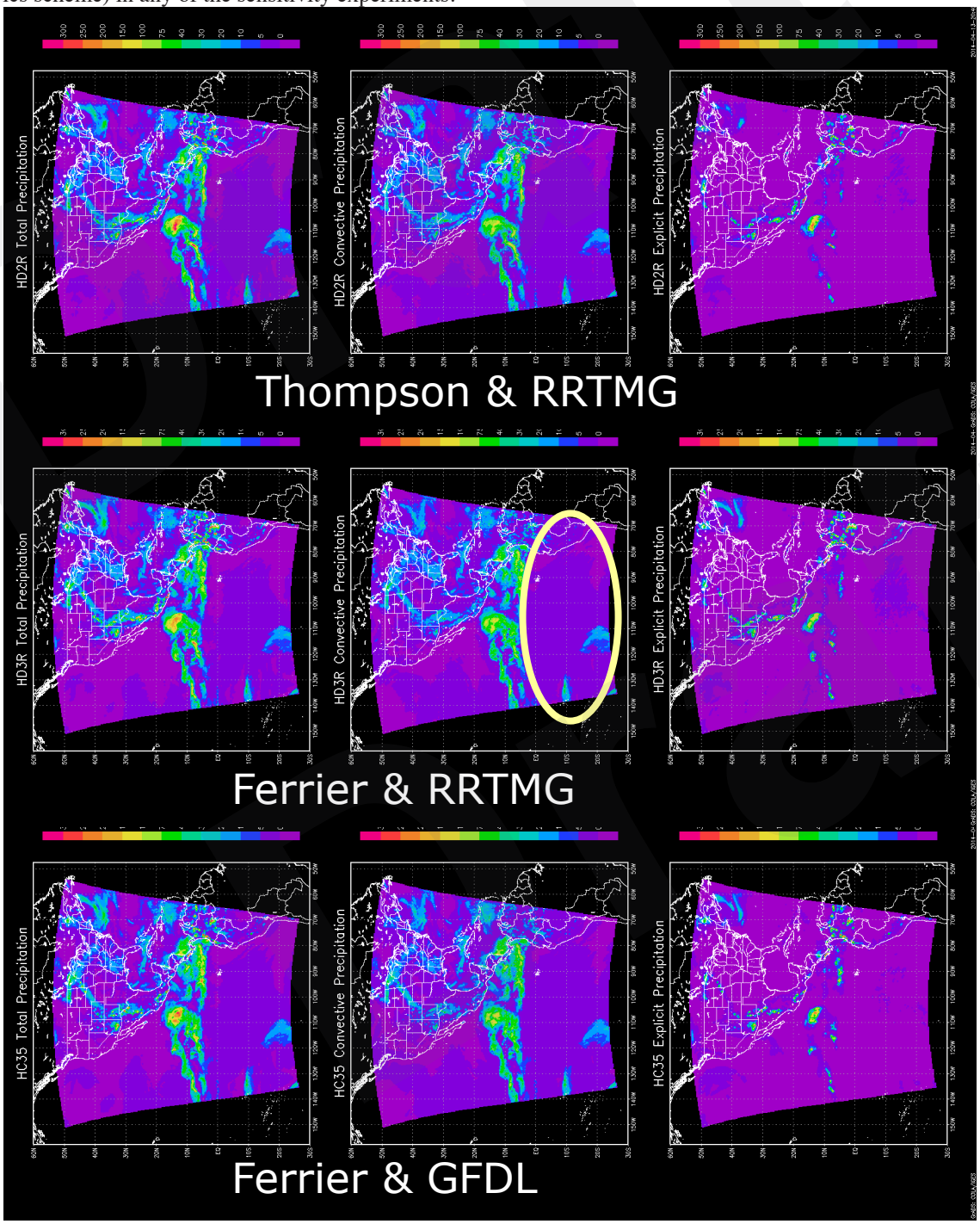

Fig. 8: 36-h HWRF forecast valid 1800 UTC 05 Jul 2012 of total precipitation (top row), which is a sum of convective precipitation (middle row) and grid-resolved precipitation (bottom row) using the operational physics, Ferrier & GFDL, (left column), Ferrier & RRTMG (middle column), and Thompson & RRTMG (right column).

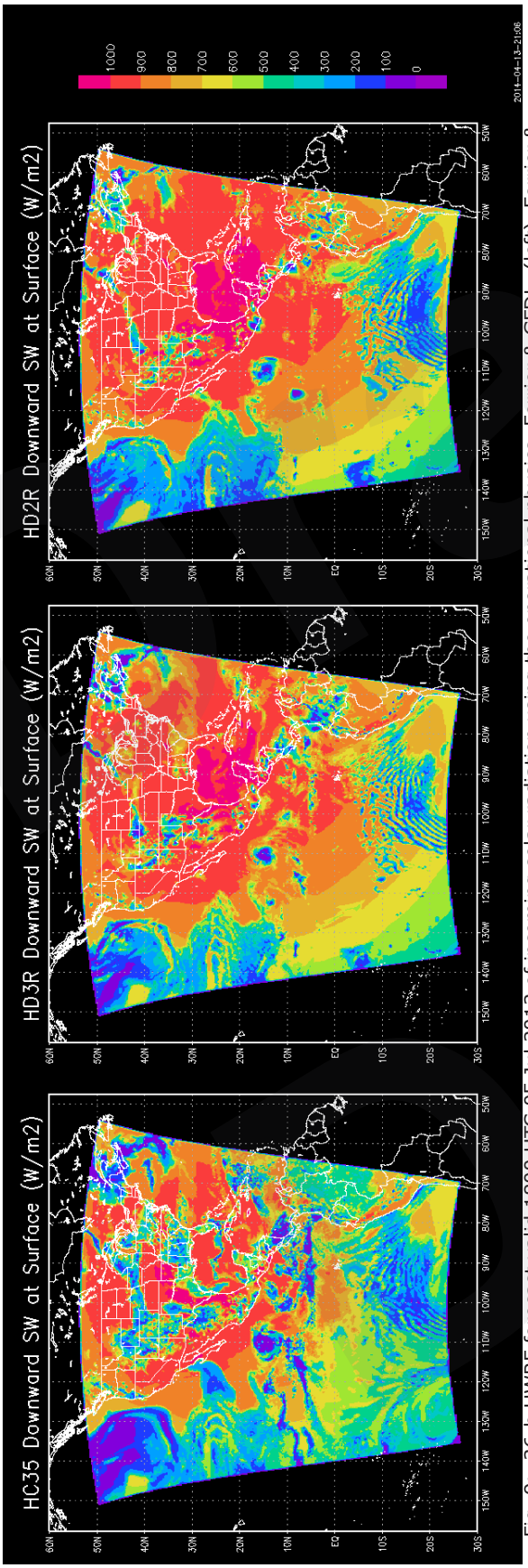

Fig. 9: 36-h HWRF forecast valid 1800 UTC 05 Jul 2012 of incoming solar radiation using the operational physics, Ferrier & GFDL, (left), Ferrier & RRTMG (middle), and Thompson & RRTMG (right).

The Smoking Gun

An investigation of the solar radiation reaching the ground (Fig. 9) in the same places that have explicit and convective precipitation led to the most important clue yet: when running RRTMG radiation scheme, much more radiation, unattenuated, reaches the ground than when using GFDL. Why? Because the RRTMG scheme is treating only the grid-resolved, explicitly-produced clouds (by the microphysics scheme) whereas the GFDL scheme is also performing radiation calculations from the unresolved convective clouds assumed through a connection with the SAS scheme. Otherwise, how could the circled region in Fig. 8 show effectively zero cloud attenuation in this region when using RRTMG as compared to using GFDL, seen here in Fig. 9. An alternative view that conveys the same basic results is found in Fig. 10 (next page) along with a new sensitivity experiment in which the SAS convective precipitation amount to create a cloud fraction scheme used by GFDL was disabled by changing a single line of code (module_ra_hwrf.F). The relationship of convective precipitation to cloud fraction is attributed by Brad Ferrier to Slingo (1989), however, no further investigation into the subsequent treatment of a cloud fraction into GFDL's radiative parameterization was pursued. ***Summary: SAS convective parameterization creates a cloud fraction amount that GFDL radiation uses to attenuate incoming solar radiation and emit longwave radiation that is entirely lacking when switching to RRTMG radiation scheme.***

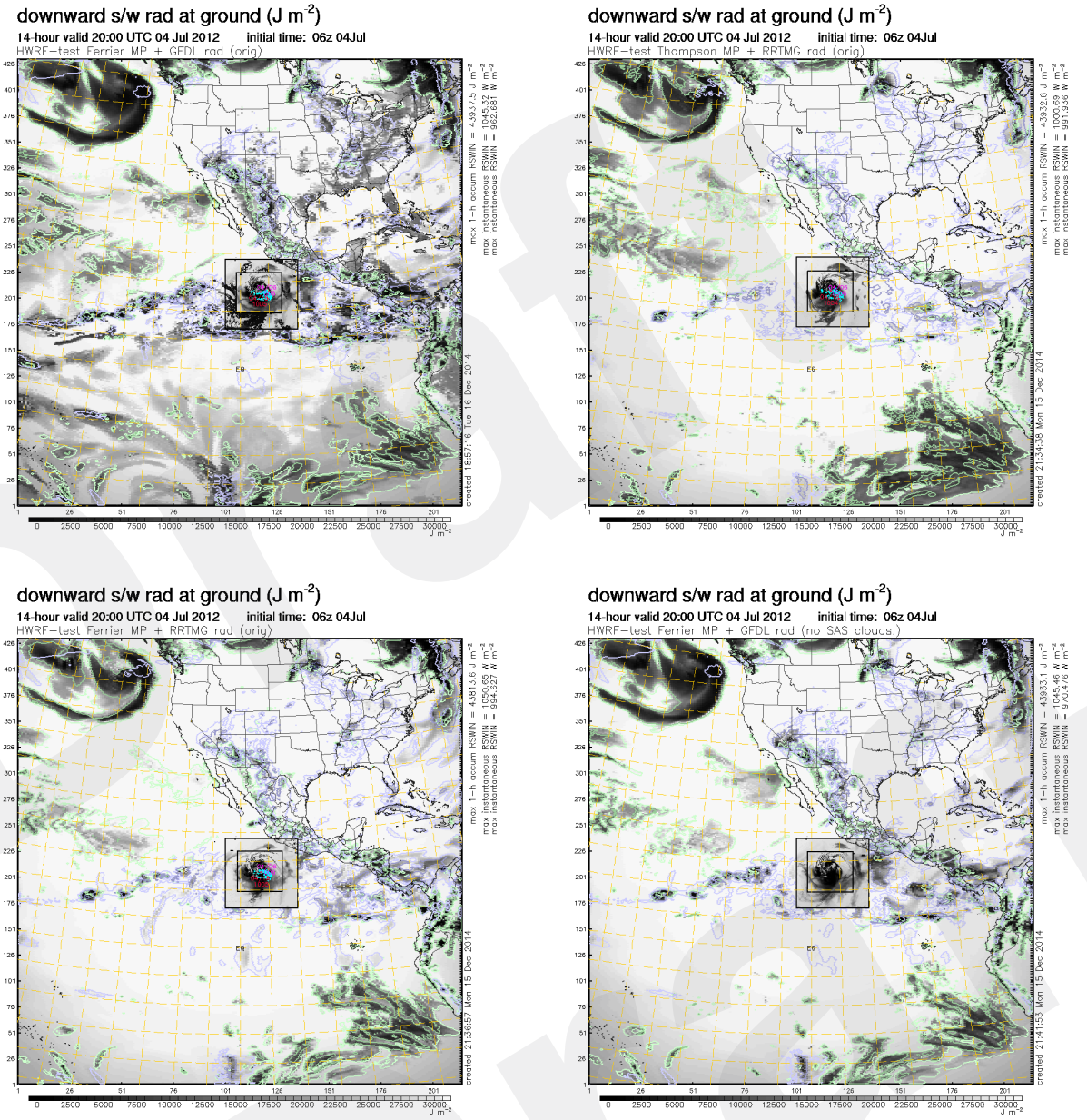

Fig. 10: 14-h HWRF forecast valid 2000 UTC 04 Jul 2012 of 1-h accumulated incoming solar radiation using the operational physics Ferrier & GFDL (top-left), Thompson & RRTMG (top-right), Ferrier & RRTMG (lower-left), and Ferrier & GFDL after disabling the SAS-derived cloud fraction (lower-right). The gray shades represent amount of 1-h accumulated incoming solar radiation* and un-shaded regions represent full sunshine whereas the deeper gray shades represent more clouds (think of it like casting a cloud shadow). On the nested domains 2 and 3, the gray shades are instantaneous incoming solar radiation reaching the ground, not 1-h accumulations, scaled linearly from zero to 1000 W m^{-2}. Solid green contours represent column-integrated liquid water content (mm), instantaneous at the valid time, and solid blue contours represent column-integrated ice (and snow). Clearly the grid-resolved clouds, explicitly by the microphysics scheme cause attenuated solar radiation seen in all 4 panels. However, note plenty of locations not enclosed by either green or blue contours in the South Pacific Ocean only found in the top-left panel (Ferrier & GFDL). When the SAS convective parameterization derived amount of cloud fraction used by the GFDL radiation was disabled entirely, those attenuated solar radiation regions are no longer found and these results are hardly different from the RRTMG scheme when using either Ferrier or Thompson microphysics scheme.

*The values of 1-h accumulated incoming solar radiation reaching the surface are incorrect. There is a bug in HWRF, being addressed by Sam Trahan, for accumulated radiation variables. It is a diagnostic variable ONLY and does not affect any outcome of the simulation. The same variables in WRF-ARW are correct.

Cloud Fraction Schemes

It is now clear that SAS convection scheme's output of precipitation amount can be interpreted into a cloud fraction by the GFDL radiation parameterization to affect incoming solar radiation (as well as longwave radiation, not shown). Furthermore, we've shown that RRTMG currently has no apparent knowledge of sub-grid-scale clouds, although there are some researchers, e.g., K. Alapaty @EPA who has investigated coupling the Kain-Fritch scheme to RRTMG. Even if the RRTMG scheme was modified to take the same SAS convective precipitation to diagnose a cloud fraction, we speculate that not all sub-grid clouds would be properly captured. For example, refer back to the satellite image in Fig. 6 and note the extensive stratus and stratocumulus cloud decks west of the California coast. The GFDL radiation scheme has essentially no recognition of these clouds because SAS must not be producing any convective precipitation in this region. Many researchers would immediately point to the need for a shallow convection scheme, but we will show next that a far simpler potential alternative using only a simplistic cloud fraction scheme may suffice. For example, Mocko and Cotton (1995) tested numerous cloud fraction schemes with varying degrees of complexity in the CSU-RAMS model. We decided to follow their method of including two schemes, specifically one by Kvamsto (1991) and another by Sundqvist et al. (1989). These scheme are very similar and extremely easy to implement so we adopted them for use in GFDL radiation as a single line of code replacing the SAS-convection cloud fraction scheme. Fig. 11 below is equivalent to the top-left panel of Fig. 10, both using Ferrier microphysics together with GFDL radiation, but substituting Kvamsto (1991) cloud fraction scheme (left side of figure) for the one attributed to Slingo (1989) that utilizes the SAS convective precipitation amount. This gave an overall result that subjectively appears "too cloudy," particularly in the South Pacific Ocean as compared to the satellite imagery. Therefore, we tried the alternative Sundqvist et al. (1989) cloud fraction scheme (right side of figure), combined with a first-guess "scale-aware" relatively humidity threshold that requires higher humidity values to make sub-grid clouds as the HWRF grid resolution increases. Note how much better either scheme produces the clouds west of CA, but the S. Pacific Ocean has more clear-sky regions using the latter cloud fraction scheme and subjectively agrees better with satellite imagery. What is more stunning to see in the images below is that the introduction of a very simple cloud fraction scheme has caused grid-resolved explicit clouds (liquid) to form in the stratus and stratocumulus regions off the west coast of North and South America. No modification to water vapor or explicit cloud variables was made, only the ***incorporation of partial cloudiness into the shortwave and longwave radiation treatment that subsequently causes the explicit microphysics scheme to produce its own clouds***.

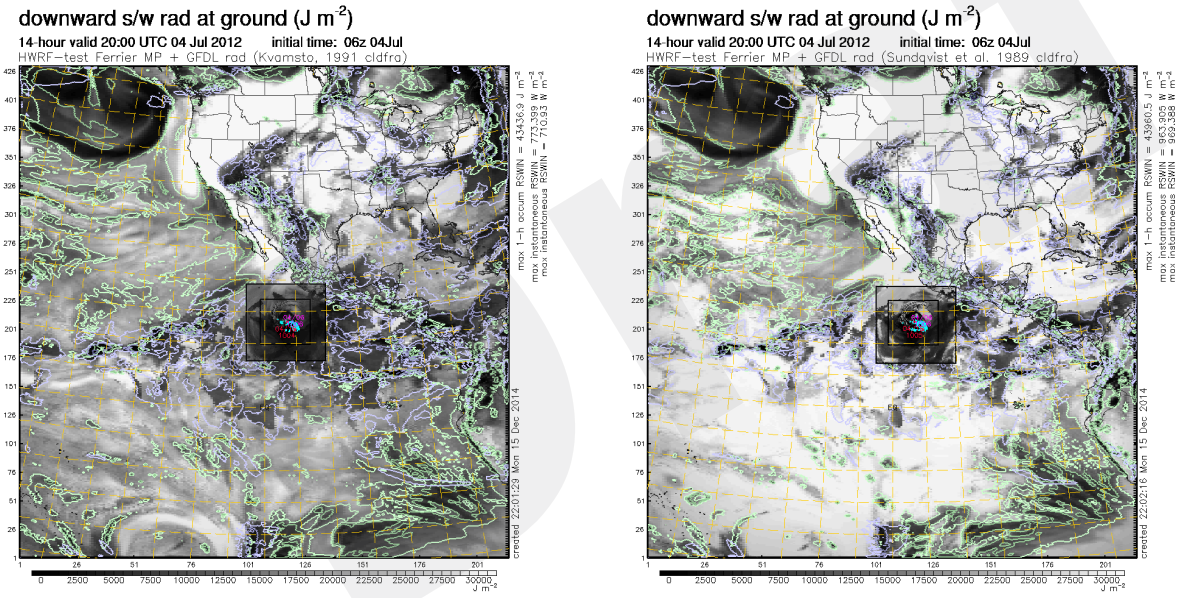

Fig. 11: Same as Fig. 10 top-left panel but replacing the SAS-derived cloud fraction scheme with a relative-humidity based cloud fraction following (Kvamsto (1991) in left panel and Sundqvist et al. (1989) in right panel. Note in particular the amount of cloudiness in S. Pacific Ocean and the creation of explicit water clouds (LWP in green contours) especially off the west coast of North America.

Next: Sub-grid Clouds into RRTMG

If RRTMG is planned as the eventual replacement of GFDL radiation parameterization in HWRF, then we must give it some sub-grid clouds. The existing WRF RRTMG scheme has a cloud fraction scheme attributed to Xu and Randall (1996), however, in practice, the scheme produces a binary 0% or 100% cloud fraction based on the absence or presence of explicit cloud condensate by the microphysics scheme. Therefore we implemented the Sundqvist et al. (1989) cloud fraction scheme into RRTMG (using WRF namelist.input change to ICLOUD=3, rather than a value of one). A complicating matter with existing RRTMG code as compared to GFDL is the requirement that liquid and ice water paths of the cloud condensate must be used to calculate cloud optical depth and subsequent radiation fluxes. Therefore, a temporary amount of cloud water or cloud ice is created solely for use by the radiation scheme, based on the thermodynamic profile and moist adiabatic ascent, reduced by an entrainment factor. These temporary values are used only in the absence of existing cloud condensate and only by the radiation scheme. Explicit and assumed LWP and IWP combined are considered in radiation fluxes but entirely ignored by all other parts of the NWP model, which only considers the explicitly-predicted cloud variables. The resulting HWRF simulations with the new scheme run together with Thompson (left) and Ferrier (right).microphysics scheme are shown in Fig. 12. Now compare Fig. 12a with Figs. 11b and 10a in conjunction with the satellite image in Fig. 6. Note the extent of clouds in the east Pacific Ocean are treated far better than previously and subjectively match the satellite image better than any prior results. Unfortunately, the same explicit clouds are not as prevalent when using the Ferrier microphysics scheme (Fig. 12b), which is subject to more investigations.

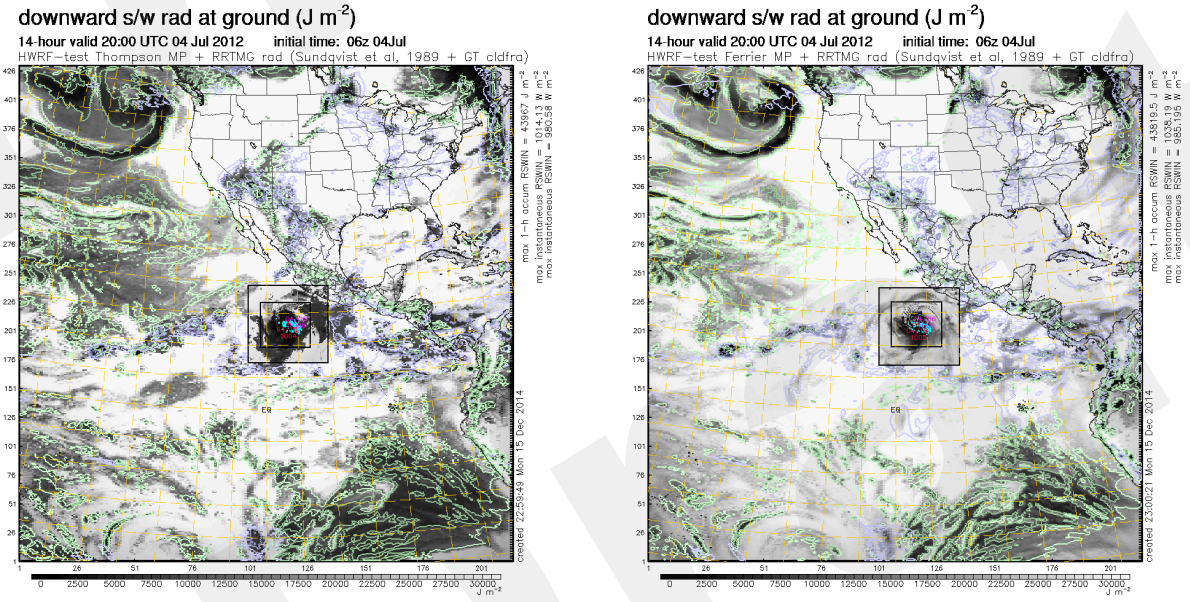

Fig. 12: Same as Fig. 11 right panel but the Sundqvist et al. (1989) cloud fraction scheme in RRTMG together with Thompson microphysics (left) and Ferrier microphysics (right).

Relation to a Known Climate Model Issue

Fig. 13 below was taken from Ma et al (2014) and clearly shows that prediction of this very same region of cloudiness is a serious problem in many climate models. Is it possible that a change in microphysics together with a partial cloudiness scheme, based on humidity alone could improve this known forecast problem area? TBD.

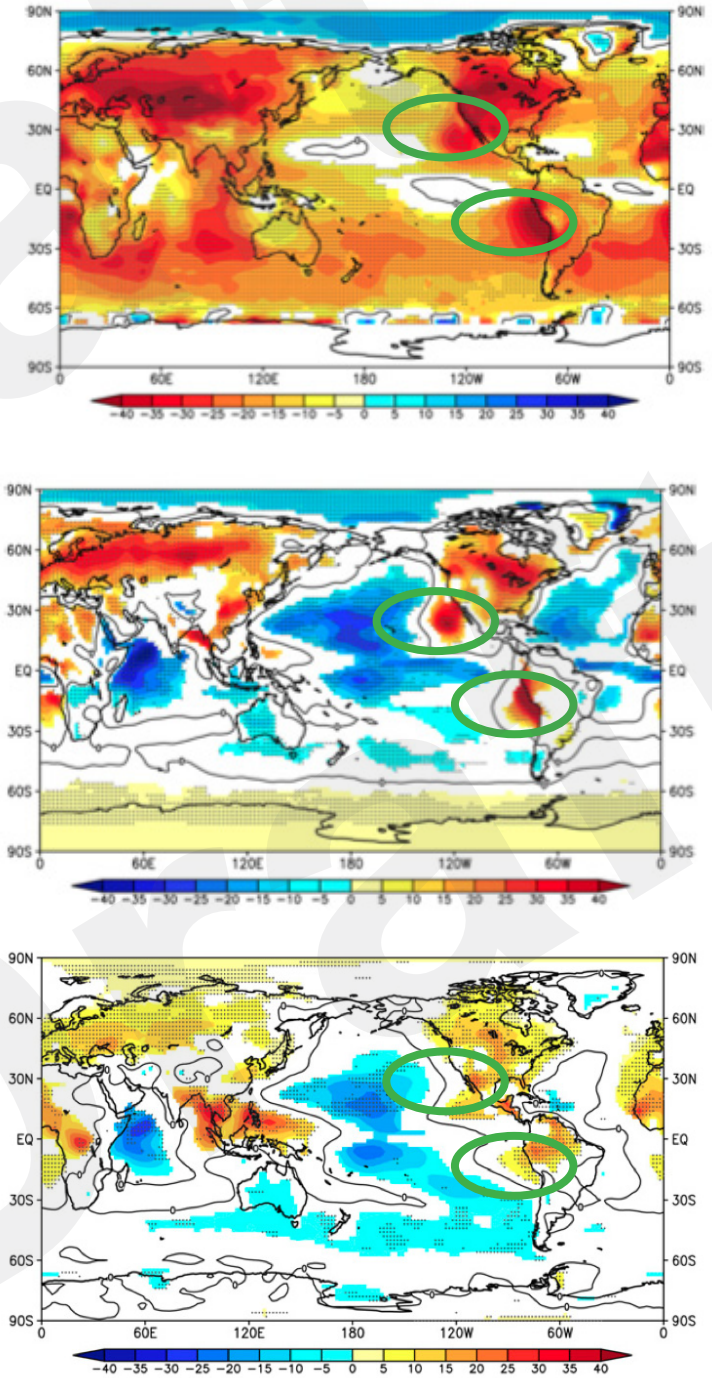

Fig. 13: Jun-Aug CMIP5 model biases of (a) cloud fraction, (b) outgoing shortwave radiation, and (c) outgoing longwave radiation [From Ma et al. 2014, Figs. 7-9].

Creating Clouds out of Thin Air

How did the clouds get created where none previously existed? Primarily longwave radiational cooling. See the following 3-hour sequence of HWRF Skew-T charts (Fig. 14) when using the original RRTMG scheme with no partial cloudiness (left) and the new test with RRTMG using the aforementioned cloud fraction scheme taken from a model grid point near the Baja California coast. It starts out subsaturated because the model initial conditions do not include clouds and the column is not fully saturated. Then, due to the supposition of clouds in the cloud fraction scheme in the nearly saturated top of PBL, longwave cooling contributes a decrease in local temperature until saturation is reached and explicit clouds are produced. One might logically ask if a better data assimilation technique could solve the problem entirely? I speculate it would not, because the effects of data assimilation rapidly dissipate after the first few hours and a sub-grid cloud scheme would still produce ongoing longwave and shortwave radiation effects that would continue to sustain clouds long after the data assimilation period ends.

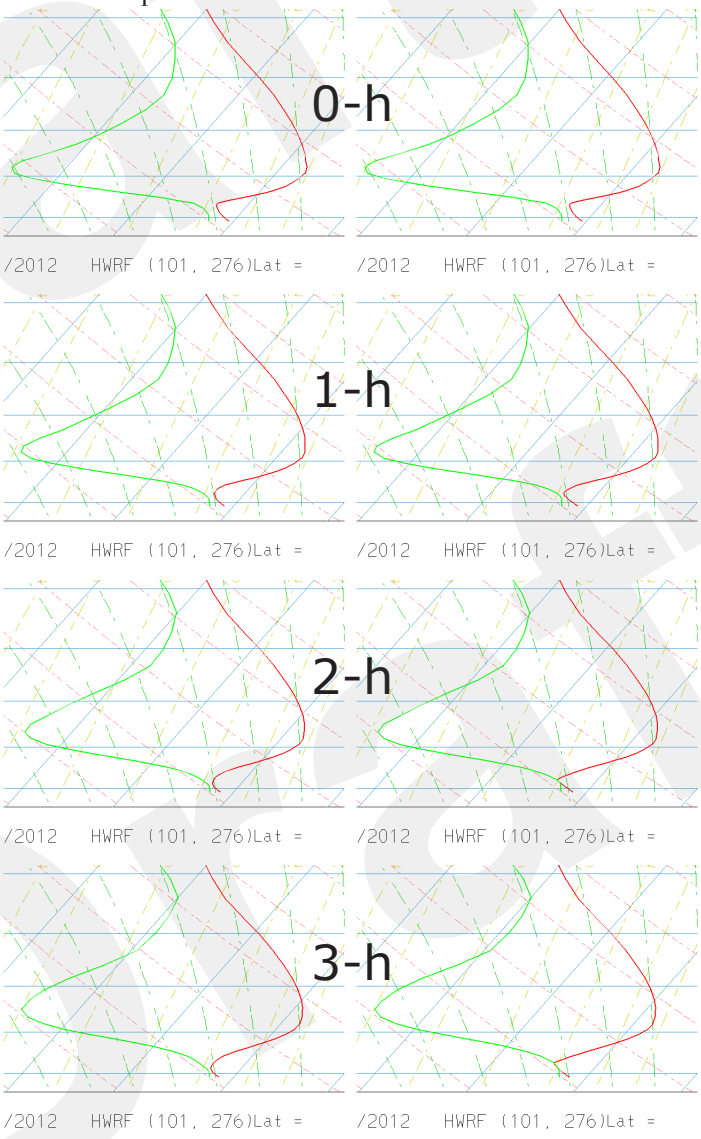

Fig. 14: Portion of a Skew-T chart for a model grid-point off the coast of Baja California at 0-, 1-, 2-, and 3-h forecast times (model initialized at 0600 UTC 04 Jul 2012) for the Daniel HWRF simulation. On the left side, the RRTMG scheme did not have fractional cloudiness while on the right side, the new fractional cloudiness scheme was used. Both sets of plots used the Thompson microphysics scheme.

Daniel Simulations

The observed and HWRF-forecast Daniel track is shown in Fig. 15 below. The HWRF tracks shown here came from the prior year simulations by DTC and used the 2013 HWRF code whereas all simulation results previously discussed in this report have used the 2014 code base with modifications as discussed. So we might expect some track changes in any sensitivity experiment solely because other model physics and bug fixes have been incorporated in the past year. However, it will be shown that many similar characteristics are found in the newer simulations.

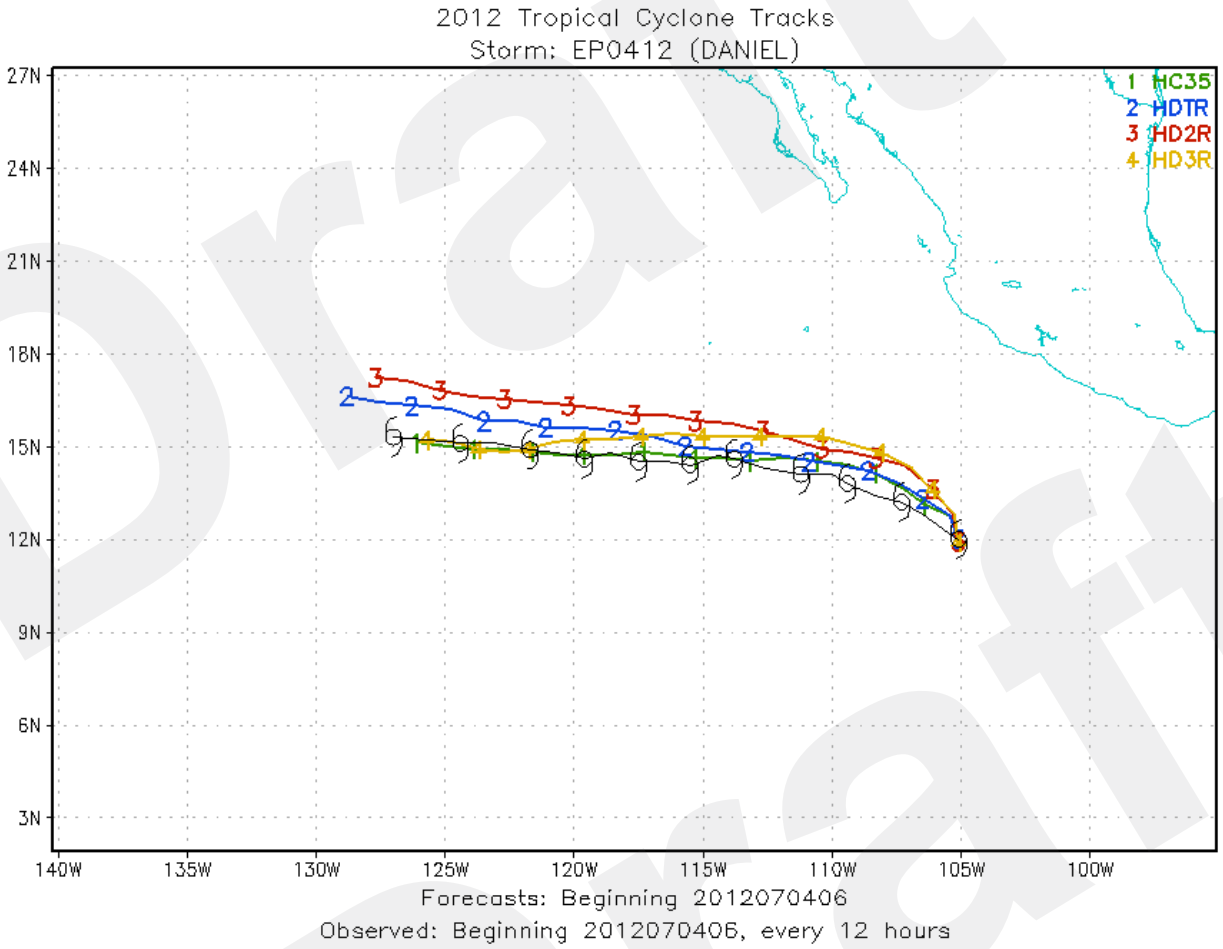

Fig. 15: Observed track (black) of Daniel and various 2013 HWRF simulations including the operational physics (green) of Ferrier and GFDL, the Thompson & RRTMG (blue and red) using two different radiation time step frequencies, and Ferrier and RRTMG (orange). In general, the Thompson scheme is too far to the right and too fast.

Daniel Simulations

Quick glimpses of the 2014 HWRF simulations of Daniel follow with daily images that are a close time match to the satellite images of Figs. 6-7 for comparison purposes in order to assist a subjective evaluation of overall cloudiness, not a particular emphasis on the tropical cyclone region, which is the subject of more analysis. Fig. 16 on this page contains the operational physics: Ferrier & GFDL. Fig. 17 on the next page contains the Thompson & RRTMG + cloud fraction scheme (left-side), and results with Ferrier & RRTMG + cloud fraction (right-side). Note in Fig. 16 how most portions of the S. Pacific Ocean contain clouds from the SAS convection scheme (not surrounded by green LWP contours) and the gradual improvement over time of the stratocumulus clouds off the west coast of N. America. In contrast, Fig. 17 shows more sporadic clouds in S. Pacific and consistent stratus-like clouds off the west coast of N. America with a decreasing tendency with time. The HWRF simulation using the same RRTMG + cloud fraction, but changing to Ferrier microphysics (Fig. 17, right-side) shows generally less clouds than the Thompson results.

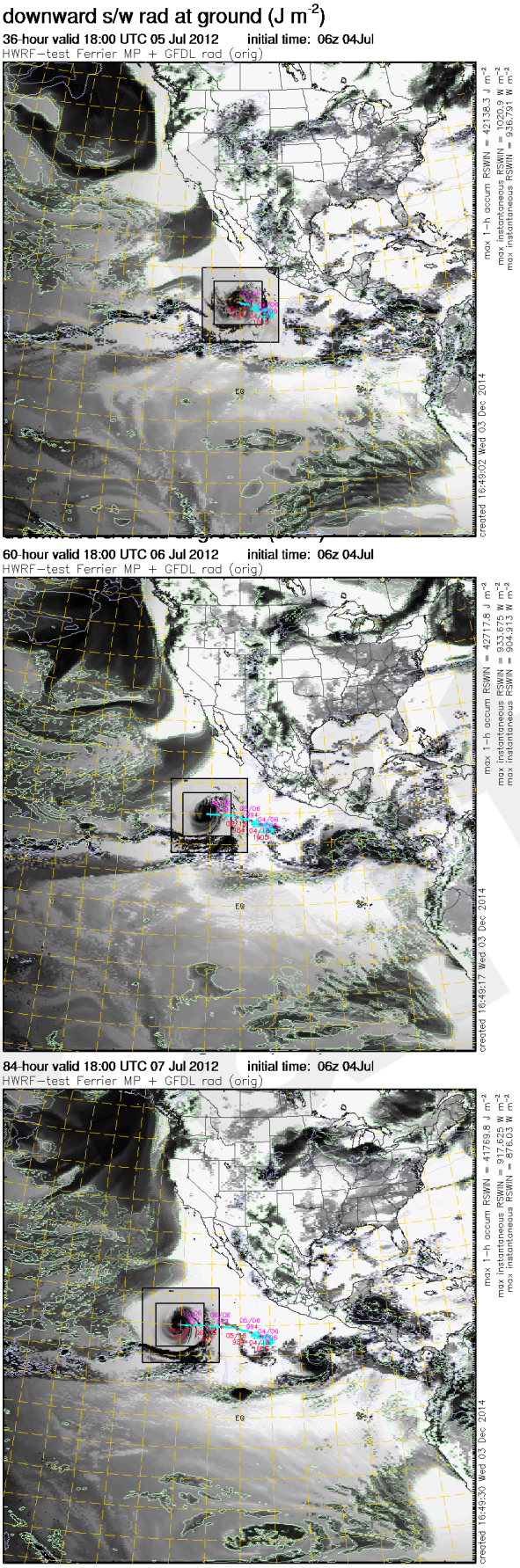

Fig. 16: Same as Fig. 10a except 36-h (top), 60-h (middle), and 84-h (bottom) HWRF Daniel forecast with operational Ferrier & GFDL schemes.

Fig. 17: [left-side on next page] Same as Fig. 16 except HWRF forecast using Thompson & RRTMG + cloud fraction scheme.

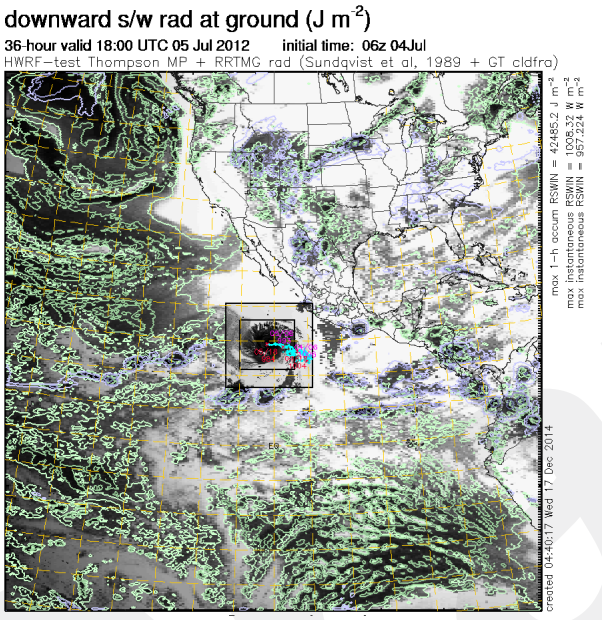
downward s/w rad at ground (J m-2)
36-hour valid 18:00 UTC 05 Jul 2012 initial time: 06z 04Jul
HWRF-test Thompson MP + RRTMG rad (Sundqvist et al, 1989 + GT cldfra)
max 1-h accum RSWIN = 42485.2 J m-2
max instantaneous RSWIN = 1008.32 W m-2
max instantaneous RSWIN = 957.224 W m-2
created 04:40:17 Wed 17 Dec 2014

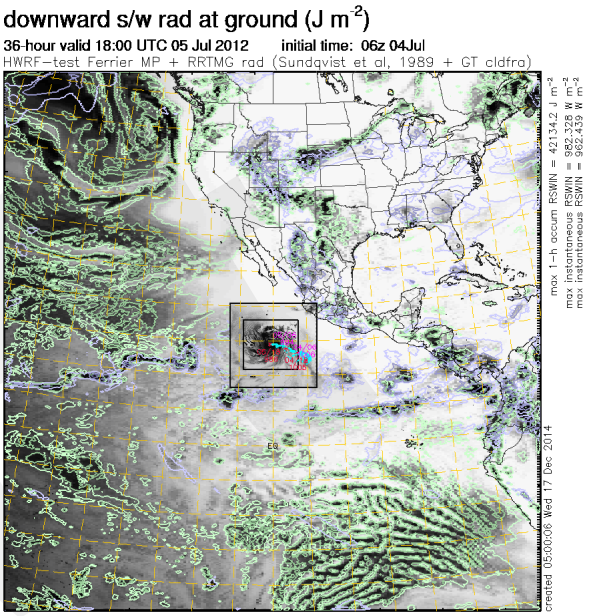
downward s/w rad at ground (J m-2)
36-hour valid 18:00 UTC 05 Jul 2012 initial time: 06z 04Jul
HWRF-test Ferrier MP + RRTMG rad (Sundqvist et al, 1989 + GT cldfra)
max 1-h accum RSWIN = 42134.2 J m-2
max instantaneous RSWIN = 982.328 W m-2
max instantaneous RSWIN = 962.439 W m-2
created 05:00:06 Wed 17 Dec 2014

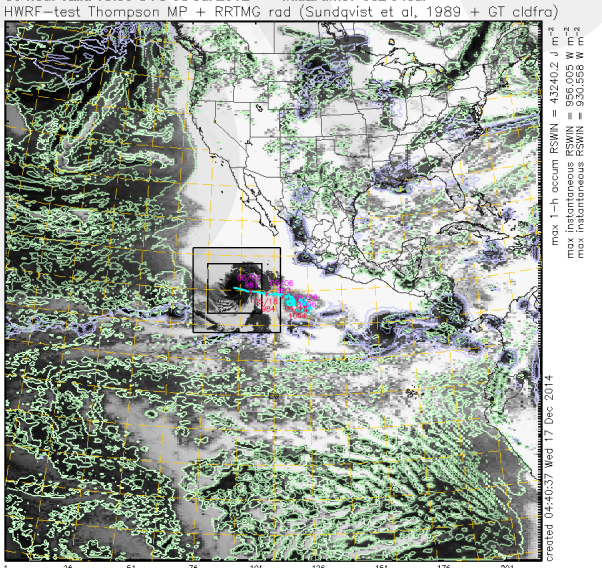
60-hour valid 18:00 UTC 06 Jul 2012 initial time: 06z 04Jul
HWRF-test Thompson MP + RRTMG rad (Sundqvist et al, 1989 + GT cldfra)
max 1-h accum RSWIN = 43240.2 J m-2
max instantaneous RSWIN = 956.005 W m-2
max instantaneous RSWIN = 930.558 W m-2
created 04:40:37 Wed 17 Dec 2014

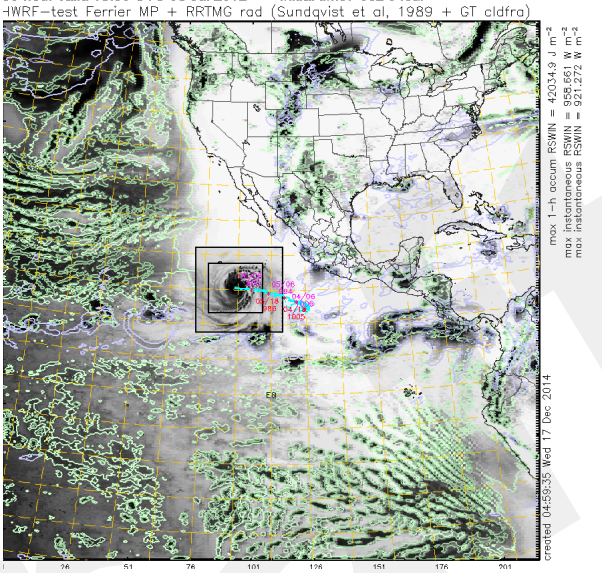
60-hour valid 18:00 UTC 06 Jul 2012 initial time: 06z 04Jul
HWRF-test Ferrier MP + RRTMG rad (Sundqvist et al, 1989 + GT cldfra)
max 1-h accum RSWIN = 42034.9 J m-2
max instantaneous RSWIN = 958.661 W m-2
max instantaneous RSWIN = 921.272 W m-2
created 04:59:36 Wed 17 Dec 2014

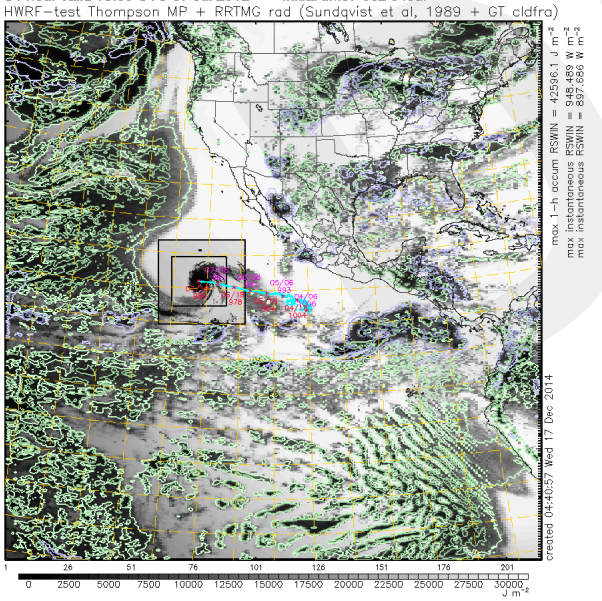
84-hour valid 18:00 UTC 07 Jul 2012 initial time: 06z 04Jul
HWRF-test Thompson MP + RRTMG rad (Sundqvist et al, 1989 + GT cldfra)
max 1-h accum RSWIN = 42596.1 J m-2
max instantaneous RSWIN = 948.489 W m-2
max instantaneous RSWIN = 897.686 W m-2
created 04:40:57 Wed 17 Dec 2014
0 2500 5000 7500 10000 12500 15000 17500 20000 22500 25000 27500 30000
J m-2

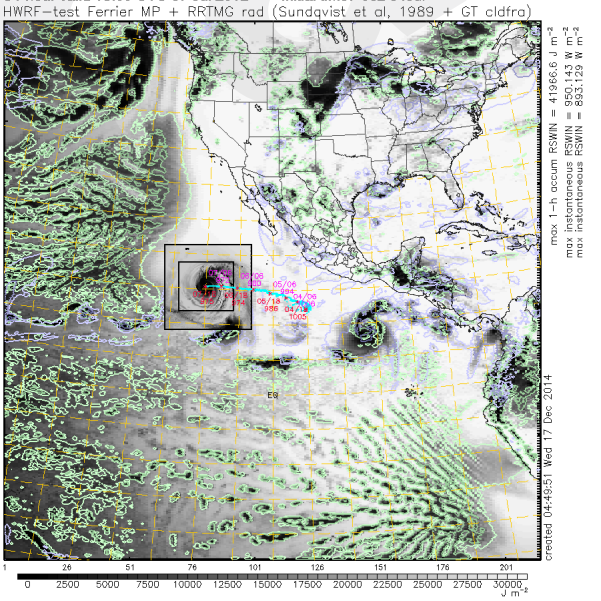
84-hour valid 18:00 UTC 07 Jul 2012 initial time: 06z 04Jul
HWRF-test Ferrier MP + RRTMG rad (Sundqvist et al, 1989 + GT cldfra)
max 1-h accum RSWIN = 41966.6 J m-2
max instantaneous RSWIN = 950.143 W m-2
max instantaneous RSWIN = 893.129 W m-2
created 04:49:51 Wed 17 Dec 2014
0 2500 5000 7500 10000 12500 15000 17500 20000 22500 25000 27500 30000
J m-2

Daniel Track

The HWRF simulated track of Daniel near the end of one forecast cycle (108-h) is shown in Fig. 18 using the different combinations of physics and continues to show the simulation using Thompson microphysics moving Daniel too fast as compared to observations. Both simulations using Ferrier are slower and nearer to 15-deg north latitude, which is likely a better solution.

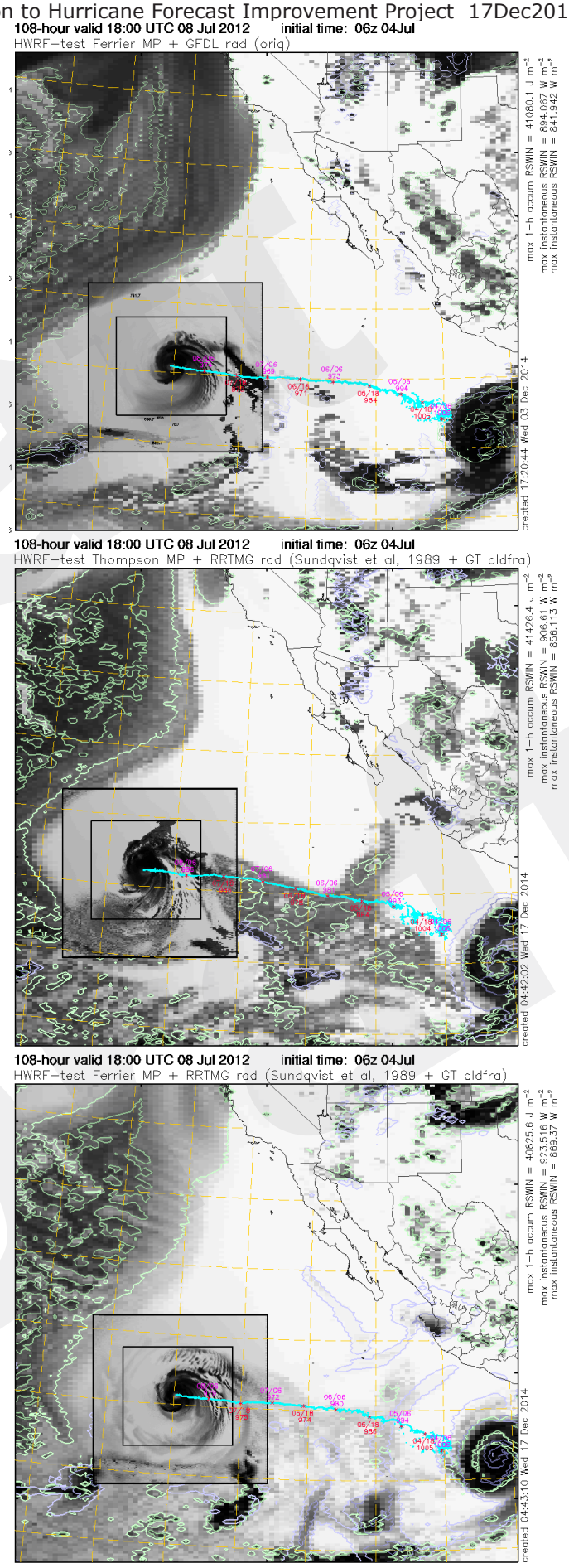

Fig. 18: 108-h HWRF forecast valid at 1800 UTC 08 Jul 2012 using operational Ferrier & GFDL (top), Thompson & RRTMG + cloud fraction scheme (middle), and Ferrier & RRTMG + cloud fraction scheme (bottom).

Next Steps

The new cloud fraction scheme combined with RRTMG is being incorporated into WRF-ARW and HWRF this month with a public release in Spring 2015 as part of the next regular release of WRF (v3.7) and HWRF (Summer 2015). The newly coupled code is now being run in a larger suite of test cases to see if there are general improvements in all ocean basins to improve tropical cyclone track and intensity characteristics. Much of the material in this document will become part of a journal paper, currently being prepared for submission in Feb. or Mar. 2015. Besides these HWRF Daniel simulations, nearly identical tests of Hurricane Sandy (2012) have already been performed. Tests of the new codes with Thompson microphysics have been run on two OU-CAPS (like) 4-km grid spacing WRF-ARW simulations, 48-h duration to test the scale-aware relative humidity threshold in the cloud fraction scheme at higher resolution and dominantly over land in conditions of typical mid-continental convective cases (2013May08 and 2013May18). Additionally, a 72-h WRF-ARW simulation of the large winter cyclone on 31 Jan to 02 Feb 2011 has been performed. Initial indications from these high resolution runs indicate a positive step in producing more clouds in a manner similar to the stratocumulus clouds off the west coast of N. America using the new cloud fraction scheme. The combination of more overall cloud cover and reduced solar radiation reaching the ground causes the model forecast to match observations better. More complete analysis is underway as part of two journal papers currently in preparation.

Overall Summary

- While the SAS convective scheme produces surrogate cloud fraction used by GFDL, it helps to capture some clouds not predicted by the grid-resolved explicit microphysics scheme, but it does not markedly improve the forecast of shallow stratus and stratocumulus clouds.
- The existing, old, RRTMG implementation in WRF does not currently treat cloud fraction in any meaningful manner, although RRTMG clearly demonstrates physically-correct mechanisms of long-wave cloud-top cooling and solar warming of existing cloud condensate.
- A newly implemented and simple (RH-based) cloud fraction scheme, together with RRTMG shows significant promise to capture large-scale regions of stratocumulus clouds.
- ***Incorporation of partial cloudiness into the shortwave and longwave radiation treatment subsequently caused the explicit microphysics scheme to produce its own clouds!***
- The new cloud fraction scheme is independent of any convection OR microphysics parameterization, although care would be needed if the BMP chosen already has some form of internal cloud fraction..
- The new cloud fraction scheme has a very preliminary method for grid scale awareness, although more systematic testing could improve this aspect simply using statistical techniques.
- The newly coupled RRTMG and Thompson radiative effective radii of cloud water, cloud ice, and snow is the only physics combination currently capable of radiative-cloud "indirect effects" (and associated aerosol-indirect effects). However, the template is already built for other BMP schemes to pass effective radii from BMP to RRTMG.

Acknowledgements

The DTC is gratefully acknowledged for funding this research. The DTC is funded by NOAA, the Air Force Weather Agency, the National Science Foundation, and the National Center for Atmospheric Research. This work was partially supported by HFIP.

References

Bretherton, C. S., T. Uttal, C. W. Fairall, S. E. Yuter, R. A. Weller, D. Baumgardner, K. Comstock, R. Wood, and G. B. Raga, 2004: The Epic 2001 Stratocumulus Study. *B. Amer. Meteorol. Soc.,* **85,** 967–977.

Bu, Y. P., R. G. Fovell, and K. L. Corbosiero, 2014: Influence of Cloud–Radiative Forcing on Tropical Cyclone Structure. *J. Atmos. Sci.,* **71,** 1644–1662.

Clement, A. C., R. Burgman, and J. R. Norris, 2009: Observational and Model Evidence for Positive Low-Level Cloud Feedback, *Science,* **325,** 460–464.

Gopalakrishnan, S., Q. Liu, T. Marchok, D. Sheinin, N. Surgi, R. Tuleya, R. Yablonsky, and Z. Zhang, 2010: Hurricane Weather Research and Forecasting (HWRF) model scientific documentation. L. Bernardet, Ed., NOAA/ Earth System Research Laboratory, 75 pp.

Kim, H.-S., C. Lozano, V. Tallapragada, D. Iredell, D. Sheinin, H. L. Tolman, V. M. Gerald, and J. Sims, 2014: Performance of Ocean Simulations in the Coupled HWRF–HYCOM Model. *J. Atmos. Oceanic Technol.,* **31,** 545–559.

Iacono, M.J., E.J. Mlawer, S.A. Clough and J.-J. Morcrette, 2000: Impact of an improved longwave radiation model, RRTM. on the energy budget and thermodynamic properties of the NCAR community climate mode, CCM3. *J. Geophys. Res.,* **105,** 14873-14890.

Klein, S. A., and D. L. Hartmann, 1993: The seasonal cycle of low stratiform clouds. *J. Climate,* **6,** 1587–1606.

Ma, H.-Y., and Coauthors, 2014: On the Correspondence between mean forecast errors and climate errors in CMIP5 Models. *J. Climate,* **27,** 1781–1798.

Mocko, D. M. and W. R. Cotton, 1995: Evaluation of Fractional Cloudiness Parameterizations for Use in a Mesoscale Model. *J. Atmos. Sci.,* **52,** 2884–2901.

Slingo, A., 1989: A GCM parameterization for the shortwave radiative properties of water cloud. *J. Atmos. Sci.,* **46,** 1419-1427.

Stephens, G. L., 2005: Cloud Feedbacks in the Climate System: A Critical Review, *J. Climate,* **18,** 237–273.

Sun, F., A. Hall, and X. Qu, 2011: Relationship between low cloud variability and lower tropospheric stability. *Atmos. Chem. Phys.,* **11,** 9053–9065.

Sundqvist, H., E. Berge, and J. E. Kristjánsson, 1989: Condensation and Cloud Parameterization Studies with a Mesoscale Numerical Weather Prediction Model. *Mon. Wea. Rev.,* **117,** 1641–1657.

Tallapragada, V., 2010: NCEP operational hurricane WRF (HWRF) modeling system. 11th WRF Users' Workshop, Boulder, CO, NCAR. [Available online at http://www.mmm.ucar.edu/ wrf/users/workshops/WS2010/presentations/session%202/2-2_vijay_wrf_users_workshop_2010.pdf.]

Teixeira, J., P. May, M. Flatau, and T. F. Hogan, 2008: SST sensitivity of a global ocean-atmosphere coupled system to the parameterization of boundary layer clouds, *J. Mar. Sys.,* **69,** 29–36.

Thompson, G., P.R. Field, R.M. Rasmussen, and W.D. Hall, 2008: Explicit forecasts of winter precipitation using an improved bulk microphysics scheme. Part II: Implementation of a new snow parameterization. *Mon. Wea. Rev.,* **136,** 5095–5115.